High-spin study of rotational structures in ^{72}Br

C. D. O'Leary,[1,*] R. Wadsworth,[1] P. Fallon,[2] C. E. Svensson,[3] I. Ragnarsson,[4] D. E. Appelbe,[5] R. A. E. Austin,[6] G. C. Ball,[7] J. A. Cameron,[6] M. P. Carpenter,[8] R. M. Clark,[2] M. Cromaz,[2] M. A. Deleplanque,[2] R. M. Diamond,[2] D. F. Hodgson,[7] R. V. F. Janssens,[8] D. G. Jenkins,[8] N. S. Kelsall,[1] G. J. Lane,[2] C. J. Lister,[8] A. O. Macchiavelli,[2] D. Sarantites,[9] F. S. Stephens,[2] D. Seweryniak,[8] K. Vetter,[2] J. C. Waddington,[6] and D. Ward[2]

[1]*Department of Physics, University of York, Heslington, York YO10 5DD, United Kingdom*

[2]*Lawrence Berkeley National Laboratory, Berkeley, California 94720, USA*

[3]*Department of Physics, University of Guelph, Guelph, Ontario N1G 2W1, Canada*

[4]*Lund Institute of Technology, P.O. Box, 118 S-221 00 Lund, Sweden*

[5]*CCLRC Daresbury Laboratory, Daresbury, Warrington WA4 4AD, United Kingdom*

[6]*Department of Physics and Astronomy, McMaster University, Hamilton, Ontario L8S 4M1, Canada*

[7]*TRIUMF, 4004 Wesbrook Mall, Vancouver, British Columbia V6T 2A3, Canada*

[8]*Argonne National Laboratory, 9700 South Cass Avenue, Argonne, Illinois 60439, USA*

[9]*Department of Chemistry, Washington University, St. Louis, Montana 63130, USA*

(Received 20 October 2003; published 15 March 2004)

High-spin states in $^{72}_{35}Br_{37}$ were studied using the ^{40}Ca(^{36}Ar,$3pn$) reaction. The existing level scheme has been significantly modified and extended. Evidence has been found for a spin reassignment of $-1\hbar$ to the previously observed negative-parity band, which carries implications for the interpretation of a signature inversion in this structure. One signature of the previously assigned positive-parity band is interpreted as negative parity and has been extended to $I^{\pi}=(22^{-})$ and its signature partner has been observed up to $I^{\pi}=(19^{-})$ for the first time. The remaining positive-parity band has been extended to $I^{\pi}=(29^{+})$. A sequence of states observed to $I^{\pi}=(22^{+})$ may be the signature partner of this structure. Configurations have been assigned to each of these three structures through comparisons to cranked Nilsson-Strutinsky calculations.

DOI: 10.1103/PhysRevC.69.034316 PACS number(s): 21.10.Re, 23.20.En, 23.20.Lv, 27.50.+e

I. INTRODUCTION

The $A\sim 70$ mass region has revealed a considerable amount of nuclear structure information in recent years. Much of the experimental work in this region has focused on nuclei lying at or close to the $N=Z$ line, with particular attention being paid to searches for signatures of neutron-proton pairing and investigations of shape coexistence, shape mixing, and band termination. The Br isotopes have played an important role in understanding the phenomena that have been observed in this region. For example, in ^{70}Br [1] evidence has been found which indicates that the $T=0$ neutron-proton pairing strength is weak in comparison to the $T=1$ strength at low excitation energy. While in ^{72}Br [2] the presence of unpaired band crossings and nuclear triaxiality have been reported, in ^{73}Br [3] smoothly terminating bands have been observed at high spin. These results show that the Br isotopes provide an important testing ground for nuclear structure models. The present work focuses on the detailed spectroscopy of ^{72}Br and reveals some conflicts with previous findings.

The high-spin structure of ^{72}Br has been studied in previous works [2,4–6]. A signature-split negative-parity structure had been established [2] up to $I^{\pi}=(26^{-})$ and was assigned a $\langle 2,3\rangle$ configuration. [In the cranked Nilsson-Strutinsky (CNS) formalism, configurations are labeled by the notation $\langle p,n\rangle$, where p is the number of $g_{9/2}$ protons in the configuration and n is the number of $g_{9/2}$ neutrons.] In the present study, we find evidence that all the states in both signatures of this structure should be lowered by one unit of spin. We have also extended the structure to $I^{\pi}=(29^{-})$. The reduction in spin has the effect of inverting the signature splitting, thereby causing a discrepancy with the work of Plettner *et al.* [2].

Two other previously observed bands were assumed to be signature partners, and observed up to $I=(18)$ and (21) [6]. These were tentatively assigned a $\langle 1,3\rangle$ positive-parity configuration by Plettner *et al.* [2]. However, our study suggests that the even-spin band of this pair has negative rather than positive parity. This band has now been extended up to $I^{\pi}=(22^{-})$. In addition, we have observed a new band up to $I^{\pi}=(19^{-})$, which is believed to be the odd spin signature partner to this re-assigned negative parity band. The odd-spin signature of the structure assigned [2] as $\langle 1,3\rangle$ has been extended to $I^{\pi}=(29^{+})$ in the present work. Furthermore, in the high-spin range ($I>21$) we believe that this structure has a $\langle 3,3\rangle$ configuration. A second new band has been observed up to $I^{\pi}=(22^{+})$, which is tentatively assigned as the even-spin partner of the $\langle 1,3\rangle$ configuration.

The data obtained in the present work are compared with the results of CNS calculations. These are found to have only moderate success in explaining the observed structures and their properties.

II. EXPERIMENTAL DETAILS AND DATA ANALYSIS

States in ^{72}Br were populated via the ^{40}Ca(^{36}Ar,$3pn$)^{72}Br reaction at the Argonne National Laboratory. An ^{36}Ar beam

*Electronic address: christopher.oleary@physics.org

of energy 145 MeV from the ATLAS facility was incident upon a 390 $\mu g/cm^2$ thick ^{40}Ca target sandwiched between two strips of gold of 113 $\mu g/cm^2$ (front) and 97 $\mu g/cm^2$ (rear) thickness.

γ rays were detected using the GAMMASPHERE [7] germanium-detector array. Light charged-particle evaporates were detected in the MICROBALL [8] device surrounding the target, and neutrons were detected in the neutron shell [9] mounted at forward angles. γ-ray events detected in prompt coincidence with three protons and one neutron were used to build a three-dimensional array (cube). The trigger conditions used in the experiment were four suppressed γ rays in prompt coincidence or two suppressed γ rays in coincidence with an event in the neutron counters (the event threshold on the neutron counters being set equal to one). These data, along with the relative peak intensities, were used to establish the positions of γ rays within, and between, the various bands.

A two-dimensional (2D) array was also built using events in coincidence with three protons and one neutron. Events from detectors situated at angles $<70°$ and $>110°$ were incremented on the x axis, while those from $70° < \theta < 110°$ were incremented on the y axis. Intensities of peaks in projected spectra from each axis were measured and expressed as a directional correlation from oriented states (DCO) ratio [10], $R_{DCO} = \mathrm{Int}_{(y\ gate)}/\mathrm{Int}_{(x\ gate)}$. Spectra were generated from these 2D arrays by requiring coincidences with the lower part of each band structure. For bands 1 and 2 the 660, 763, 996, 867, and 1036 keV transitions were used, while for bands 3, 4, and 5 the 270, 353, 730, 841, and 1049 keV transitions were used. Using this information it was possible to distinguish between $I \rightarrow I-2$ (stretched quadrupole) and

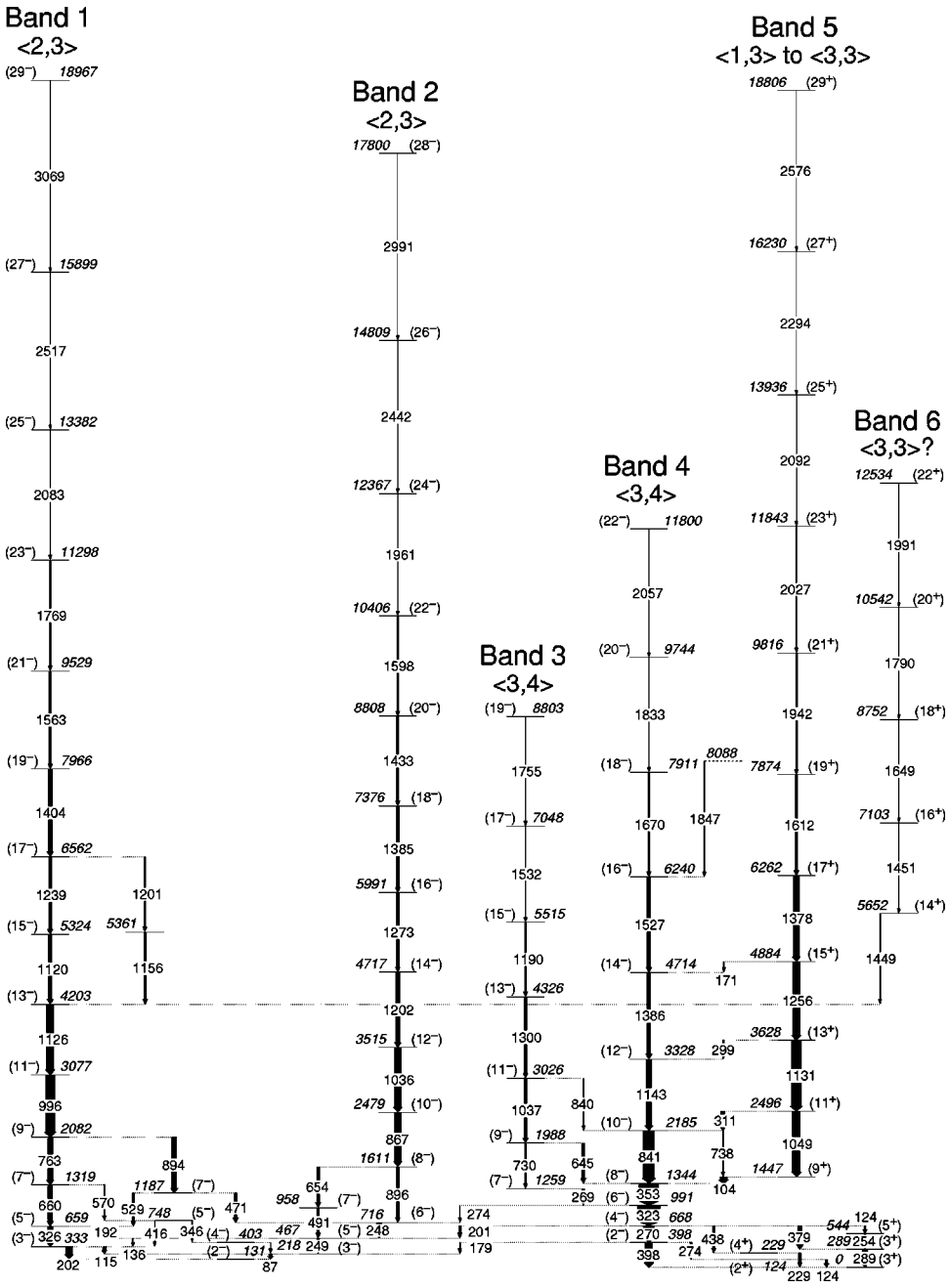

FIG. 1. Level scheme derived for ^{72}Br from the current analysis. States are labeled with assigned spin, parity, and energy. Arrow widths are proportional to γ-ray intensity. Bands have been labeled with their assigned configuration from our cranked Nilsson-Strutinsky calculations, using notation $\langle p,n \rangle$, where p is the number of $g_{9/2}$ protons in the configuration and n is the number of neutrons. All states have tentatively assigned spins and parities (bracketed) as the ground-state spin and parity have not been firmly established [4].

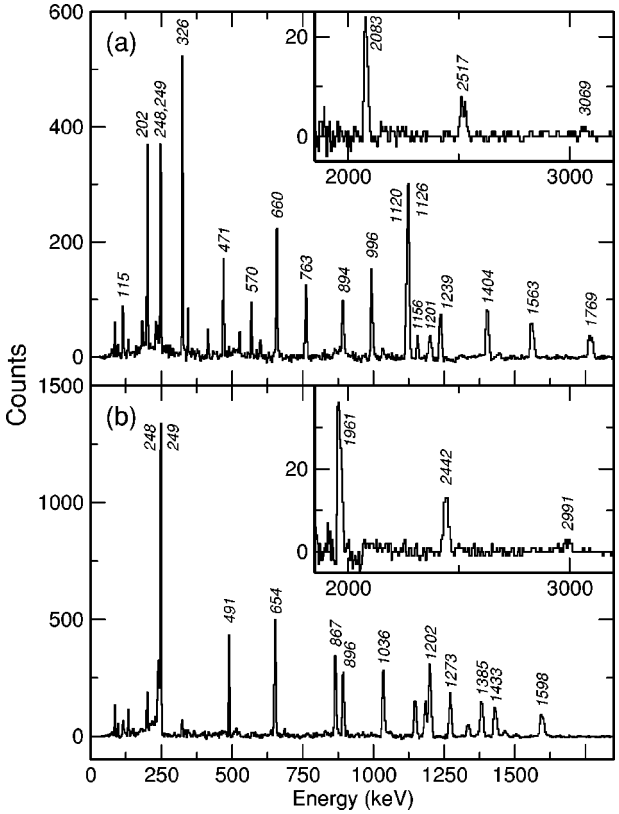

FIG. 2. γ-ray spectra for bands 1 and 2 in ^{72}Br. (a) Band 1: A sum of double gates from the cube on every combination of the 763, 996, 1156, 1239, 1404, 1563, 1769, 2083, 2517, and 3069 keV transitions. (b) Band 2: A sum of double gates from the cube on every combination of the 867, 1036, 1202, 1385, 1433, 1598, 1961, 2442, and 2991 keV transitions.

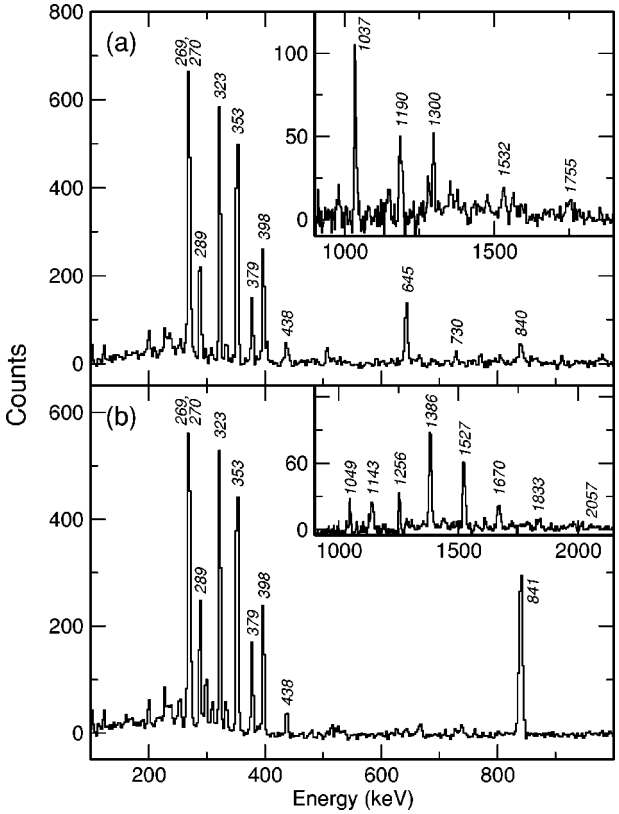

FIG. 3. γ-ray spectra for bands 3 and 4 in ^{72}Br. Band 3: A sum of double gates between the 398, 323, and 353 keV transitions and the 645, 1037, 1300, and 1190 keV transitions. Band 4: A sum of double gates between the 398, 323, and 353 keV transitions and the 1143, 1670, 1833, and 2057 keV transitions.

$I \rightarrow I-1$ (stretched dipole) transitions. Known stretched quadrupole transitions were found to have DCO values around 1.1, while stretched dipoles have a value of 0.7. Peak intensities were also measured in the full projection of each axis of the matrix and their ratio expressed in the form $A_R = \mathrm{Int}_{(\mathrm{x\ proj})}/\mathrm{Int}_{(\mathrm{y\ proj})}$. Here, stretched quadrupole transitions were found to have ratios of 0.9, while stretched dipoles have a value of 1.2.

III. RESULTS

The level scheme derived from the current analysis is shown in Fig. 1. States have been grouped into six bands (labeled 1–6). Bands 1,2 and 3,4 are believed to be signature-split rotational structures. We have also tentatively assigned bands 5 and 6 as signature partners, though the evidence for this is much weaker than in the other two cases.

γ-ray spectra obtained from double coincidence gates on the 3*pn*-gated cube are shown in Fig. 2 for bands 1 and 2, Fig. 3 for bands 3 and 4, and Fig. 4 for bands 5 and 6.

Data for transitions and energy levels shown in Fig. 1 are presented in Tables I–IV. Table I shows data for states in bands 1 and 2, Table II for those in bands 3 and 4, and information on states in bands 5 and 6 is presented in Table III. In all these tables the notation ${}_iI_n^\pi$ refers to the initial state spin and parity and ${}_fI_n^\pi$ to the populated state spin and parity. In both cases the subscript *n* refers to the order of occurrence of that spin/parity combination. Data for states which are not grouped into bands are presented in Table IV.

The level scheme of Fig. 1 represents a significant modification to previous work and the reasons for our changes are discussed below. Note that *all* states have tentative spin assignments as the ground-state spin has not been firmly established [4]. With this in mind, spin assignments have primarily been based on the experimentally measured DCO ratios given in Tables I–IV and on the assumption that the ground-state spin has $I^\pi = 3^+$.

The DCO ratios indicate a multipolarity change from previous work for several transitions. For example, the 202 keV$(3_2^- \rightarrow 2_1^-)$ transition, which was previously assigned as an $E2$ γ ray [2], is now assigned as $M1$, since it has an R_{DCO} of 0.86. Similarly, the 654 keV $(8_2^- \rightarrow 7_1^-)$ is found to have a DCO value of 0.64, which again is inconsistent with the previous $E2$ assignment.

Comparisons between γ-ray intensities for bands 1 and 2 in Table I and those for band 5 in Table III show that at low spins band 5 is populated more readily than either bands 1 or 2, and is the yrast structure to $I \sim 17$. This would be surprising if the level scheme from previous work [2] were correct as it shows bands 1 and 2 to be lower in energy than band 5. In that work no γ-ray intensity information is reported, so a

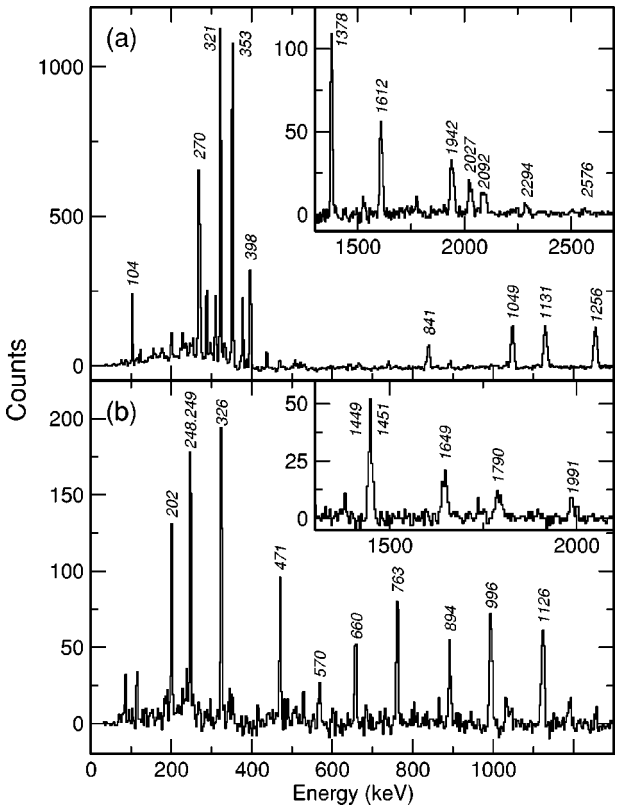

FIG. 4. γ-ray spectra for bands 5 and 6 in ^{72}Br. Band 5: A sum of double gates on every combination of the 1049, 1131, 1256, 1378, 1612, 1942, 2027, 2092, 2294, and 2576 keV transitions. Band 6: A sum of double gates on every combination of the 1449, 1451, 1649, 1790, and 1991 keV transitions added to a sum of double gates between those transitions and the 660, 793, 996, and 1126 keV transitions.

direct comparison is not possible. It should be noted that there is a potential problem in extracting the relative intensities of bands 1,2 and band 5 since they are not linked. In the present work the intensities of each of the bands were measured from double coincidence data, using all possible combinatorial γ pairs in each band. Since there are a similar number of coincident transitions in the bands, and bearing in mind the trigger and sorting conditions discussed above, one might expect the measurement method to have little effect on the relative intensities of the bands.

In order to provide further support for our assignments we have made a comparative study between excited states in ^{72}Br and other odd-odd, even-mass isotopes of bromine. These are shown in Fig. 5, where it can be seen that our interpretation (i.e., lowering the spins of bands 1 and 2 by $1\hbar$) appears to fit the systematics more readily.

A more complex comparison has been made to nuclei with the same isospin ($T=1$). The difference between the experimental mass of a nucleus and the mass calculated in a liquid drop or droplet model is referred to as the "microscopic energy" or the "experimental shell energy." This difference generally varies in the approximate range -10 MeV to 5 MeV, with the large negative values found around doubly magic nuclei. Away from closed shells, this shell energy varies smoothly as a function of neutron or proton number as seen in Figs. 1 and 2 of Möller *et al.* [16]. In these figures, the energies of nuclear ground states are compared, but one might similarly compare the energies at some fixed spin value. This quantity is also expected to vary smoothly (at least for collective rotation). One difficulty for nuclear ground states is that a pairing energy must be added so that even, odd, and odd-odd nuclei are treated on a somewhat different footing. This often leads to a "zigzag" behavior in plots of the experimental shell energy, but with increasing spin, pairing becomes less important and should be negligible at very high-spin values. Therefore, when comparing the total energy of very high-spin states, the total energy of even, odd, and odd-odd nuclei is expected to vary smoothly if the pairing energy is not included in the macroscopic energy. This was exemplified for dysprosium and erbium isotopes in Ref. [17] and will be studied in more detail in a forthcoming publication [18].

A comparison along these lines has been carried out for ^{70}Se, ^{72}Br, and ^{74}Kr in Fig. 6. These three nuclei have $N-Z=2(T=1)$ and so they should have similar values of the Wigner energy (the $|N-Z|$ dependent term in macroscopic mass models). As we are mainly interested in high-spin states, no pairing has been included in the macroscopic mass formula which corresponds to the finite-range droplet model (FRDM) of Möller *et al.* [16]. The ground states of the even nuclei are then plotted at their experimental shell energies while the ground state of the odd-odd nucleus is lifted by the pairing terms of the FRDM model relative to the standard definition for the experimental shell energy, i.e., by $\Delta_p+\Delta_n-\delta_{np}$ using the notation in Ref. [16]. This energy amounts to 2.52 MeV for ^{72}Br. The energy of the higher-spin states are then plotted relative to this even-mass FRDM reference. We note that already the $I=12$ state is built at a similar total energy for the even ^{70}Se and ^{74}Kr nuclei and the odd-odd ^{72}Br nucleus which thus shows that they have similar pairing energies and suggests that the pairing energy is more or less negligible at this spin value. We also expect that for higher-spin values, the energy should vary continuously from ^{70}Se to ^{72}Br to ^{74}Rb. Since the transition energies become quite large relative to the unevenness, it should become possible to fix the spin values in one nucleus if the spin values of its neighbors are known. Noting that in Fig. 6 the energy varies smoothly only for the full-drawn lines (corresponding to the lower-spin values of our new interpretation for bands 1 and 2 in ^{72}Br), we suggest that the level scheme shown in Fig. 1 has the correct spin values for bands 1 and 2 in ^{72}Br, and that the values presented in earlier work [2] are $1\hbar$ too high.

The spins of bands 4 and 5 remain the same as assigned in previous work. We note that band 4 is the yrast structure for $I\leqslant 10$, which seems to more readily agree with our $-1\hbar$ reassignment to bands 1 and 2. There are several transitions connecting bands 3 and 4, and bands 4 and 5 at low spins. It had previously been assumed that band 4 was the positive-parity signature partner to band 5, but the similarity in energy-level systematics, coupled with the cross-talk between bands 3 and 4, leads to the suggestion that they are signature partners.

The spin assignment of band 6 is somewhat tentative. It feeds into the 13^- state of band 1 through a transition of 1449 keV. This band is populated very weakly, and so it is

TABLE I. Spins, γ-ray and level energies, intensities of γ rays with initial state energy, and spin and populated state spin for bands 1 and 2. The energies are given in keV.

${}_iI_n^\pi$	$E_{\rm lvl}$	E_γ	±	I_γ	±	${}_fI_n^\pi$	$R_{\rm DCO}$	±	$A_{\rm R}$	±
(3_2^-)	333	201.8	0.1	28.8	3.4	(2_1^-)	0.86	0.06	1.01	0.09
		115.1	0.1	12.5	1.4	(3_1^-)	0.76	0.04	1.30	0.05
(5_2^-)	659	192.2	0.1	2.2	0.1	(5_1^-)				
		325.8	0.1	26.2	1.1	(3_2^-)	1.14	0.06	0.93	0.07
(7_1^-)	958	490.6	0.1	10.1	0.5	(5_1^-)	1.03	0.04	0.96	0.02
(7_4^-)	1319	570.3	0.1	6.3	0.3	(5_3^-)	1.33	0.07	0.88	0.03
		659.8	0.1	18.1	0.7	(5_2^-)	1.92	0.08	0.90	0.02
(8_2^-)	1611	653.6	0.1	13.2	0.5	(7_1^-)	0.64	0.03	1.25	0.02
		895.7	0.1	9.9	0.4	(6_1^-)	1.30	0.03	0.89	0.02
(9_2^-)	2082	763.2	0.1	21.4	0.8	(7_4^-)	1.25	0.03	0.55	0.02
		894.0	0.1	21.9	0.7	(7_2^-)	1.05	0.21	0.89	0.02
(10_2^-)	2479	867.3	0.1	27.8	0.9	(8_2^-)	1.23	0.05	0.97	0.03
(11_2^-)	3077	995.8	0.1	40.4	1.3	(9_2^-)	0.83	0.09	0.91	0.02
(12_2^-)	3515	1036.4	0.1	27.7	1.0	(10_2^-)	1.07	0.03	0.98	0.02
(13_1^-)	4203	1126.0	0.1	31.1	1.1	(11_2^-)				
(14_2^-)	4717	1202.3	0.1	19.2	0.7	(12_2^-)	1.30	0.03	0.80	0.01
(15_1^-)	5324	1120.3	0.1	16.5	0.7	(13_1^-)				
(16_1^-)	5991	1273.3	0.1	10.4	0.4	(14_2^-)	1.40	0.07		
(17_1^-)	6562	1201.3	0.1	6.5	0.3	$(?_?^?)$			0.80	0.01
		1238.9	0.1	12.5	0.5	(15_1^-)			0.69	0.03
(18_1^-)	7376	1384.7	0.1	9.9	0.4	(16_1^-)				
(19_1^-)	7966	1404.1	0.1	17.9	0.6	(17_1^-)	1.03	0.04	1.24	0.03
(20_1^-)	8808	1432.5	0.1	8.9	0.4	(18_1^-)				
(21_1^-)	9529	1563.0	0.1	10.1	0.4	(19_1^-)	0.99	0.04	0.96	0.02
(22_1^-)	10406	1597.7	0.1	7.6	0.3	(20_1^-)			1.11	0.03
(23_1^-)	11298	1769.0	0.1	6.2	0.3	(21_1^-)	0.95	0.02	0.95	0.02
(24_1^-)	12367	1961.2	0.2	2.5	0.2	(22_1^-)			1.05	0.03
(25_1^-)	13382	2083.4	0.2	3.5	0.2	(23_1^-)				
(26_1^-)	14809	2441.7	0.5	1.1	0.1	(24_1^-)			1.17	0.04
(27_1^-)	15899	2516.9	0.8	0.9	0.1	(25_1^-)			1.08	0.04
(28_1^-)	17800	2991.0	1.3	0.1	0.0	(26_1^-)				
(29_1^-)	18967	3068.6	1.8	0.3	0.0	(27_1^-)				

unlikely that the 5652 keV state has $I>14$ as it would make band 6 compete favorably with band 5. The assignment of band 6 as the signature partner to band 5 is largely due to the CNS calculations (discussed below).

The residual Doppler shift attenuation method [21] was used to plot curves of F_τ versus γ-ray energy. Two spectra were created using the $3pn$ particle gate and gated on the lowest few transitions of each of bands 1 and 2 in detectors in rings at (a) 70° and 79° (forward angles) and (b) 110° and 101° (backward angles) to the beam direction. The relative Doppler shifts ($\langle v\rangle$) of transitions deexciting high-spin levels in these bands at these angles were measured by determining the energy of peak centroids in these spectra ($E_{\rm back}$ and $E_{\rm forward}$). If E_0 is the energy of the centroid measured in the total projection (including detectors at all angles) with Doppler shift correction $v_{\rm corr}=0.0393c$ applied, then F_τ is given by

$$F_\tau = \frac{\langle v\rangle}{v_0} = \frac{E_{\rm back}-E_{\rm front}}{2E_0\cos(\theta)} + v_{\rm corr}, \tag{1}$$

where θ is the mean angle of the detector rings and v_0 is the initial velocity of the recoiling ^{72}Br nucleus (assumed to be $0.044c$).

Experimental F_τ values were calculated using standard stopping powers [22] for various Q_t values for bands 1 and 2. A Q_t of about 2.2 e b (which corresponds to a quadrupole deformation of $\epsilon_2=0.30$ if $\gamma=0°$ is assumed) is found for states in the $17\hbar$ to $21\hbar$ region in band 1 [see Fig. 7(a)]. There is, however, some evidence that a slightly lower Q_t value may apply to the highest spins observed in this structure. The curve for band 2 clearly falls away from the $Q_t=2.2$ curve above spin 22 [see Fig. 7(b)]. This again suggests that this band has a decreasing quadrupole moment as I in-

TABLE II. Spins, γ-ray and level energies, intensities of γ rays with initial state energy, and spin and populated state spin for bands 3 and 4. The energies are given in keV.

${}_iI_n^\pi$	$E_{\rm lvl}$	E_γ	±	I_γ	±	${}_fI_n^\pi$	$R_{\rm DCO}$	±	$A_{\rm R}$	±
(2_2^-)	398	397.9	0.1	32.5	2.5	(3_1^+)	0.88	0.03	1.06	0.03
		179.0	0.1	4.5	0.4	(3_1^-)	0.75	0.04	1.21	0.04
		274.2	1.0	10.4	0.8	(2_1^+)			0.90	0.03
(4_2^-)	668	124.0	0.1	7.1	0.3	(5_1^+)				
		201.1	0.1	7.9	0.4	(5_1^-)	0.87	0.33	1.57	0.28
		269.8	0.1	49.8	1.7	(2_2^-)	1.00	0.01	1.00	0.01
		378.5	0.1	21.0	0.7	(3_2^+)	0.64	0.03	1.15	0.02
		438.2	0.1	8.7	0.4	(4_1^+)	1.00	0.04	1.16	0.05
(6_2^-)	991	323.1	0.1	100.0	2.8	(4_2^-)	1.06	0.03	1.06	0.11
		274.2	0.2	1.6	0.2	(6_1^-)				
(7_3^-)	1259	269.0	0.1	13.3	0.8	(6_2^-)			1.00	0.01
(8_1^-)	1344	353.1	0.1	89.2	2.8	(6_2^-)	1.16	0.03	0.93	0.03
(9_1^-)	1988	644.6	0.1	12.3	0.6	(8_1^-)	0.72	0.03	0.64	0.19
		729.7	0.2	4.5	0.3	(7_3^-)	1.33	0.12		
(10_1^-)	2185	841.4	0.1	48.5	1.7	(8_1^-)	1.34	0.04	0.39	0.01
		738.1	0.2	4.3	0.3	(9_1^+)	0.68	0.06	1.15	0.03
(11_1^-)	3026	1037.2	0.2	12.7	0.7	(9_1^-)	0.81	0.11	0.98	0.02
		840.1	1.0	3.6	0.4	(10_1^-)				
(12_1^-)	3328	1143.1	0.1	24.1	0.9	(10_1^-)				
(13_2^-)	4326	1300.0	0.3	10.2	0.5	(11_1^-)	0.91	0.04	0.78	0.01
(14_1^-)	4714	1386.1	0.1	16.4	0.7	(12_1^-)				
(15_3^-)	5515	1189.5	0.8	8.1	0.4	(13_2^-)			1.05	0.01
(16_2^-)	6240	1526.7	0.1	13.7	0.6	(14_1^-)	0.81	0.23	0.98	0.02
(17_2^-)	7048	1532.4	1.0	3.5	0.3	(15_3^-)	2.26	1.42		
(18_2^-)	7911	1670.2	0.2	6.9	0.3	(16_2^-)	1.12	0.05	1.10	0.03
(19_2^-)	8803	1755.0	1.0	2.0	0.2	(17_2^-)				
(20_2^-)	9744	1833.1	0.6	1.5	0.2	(18_2^+)				
(22_2^-)	11800	2056.7	1.0	0.7	0.1	(20_2^+)				

creases. Unfortunately, it was not possible to extract reliable F_τ curves for any of the other bands.

IV. DISCUSSION

In the present work, we have compared the experimental rotational bands with the results of cranked Nilsson-Strutinsky (CNS) calculations using the modified oscillator potential. The theoretical formalism is reviewed in Ref. [23] and we have used the $A=80$ parameters of Galeriu *et al.* [24]. These calculations are carried out with no pairing which means that they should not be used for detailed comparisons with experiment at very low-spin values. Indeed, the calculated equilibrium configurations are oblate or near-oblate at low and intermediate spin. We will however concentrate on spin values higher than $I\sim 12$, where collective configurations with near-prolate equilibrium shapes are calculated to be lowest in energy. These configurations evolve towards noncollective oblate shapes when they approach their maximum spin values, $I\sim 30$.

Configuration assignments have been made to the six bands in ^{72}Br through a comparison of experimental energies minus a rigid rotor reference energy **(**$0.02594[I(I+1)]$**)** as a function of spin [Fig. 8(a)], with the equivalent information from CNS calculations, see Fig. 8(b). For bands 1 and 2 the previous [2] $\langle 2,3\rangle$ configuration is retained, while a $\langle 3,4\rangle$ configuration seems most plausible for bands 3 and 4. Band 5 appears to evolve from a $\langle 1,3\rangle$ configuration at low spin to a $\langle 3,3\rangle$ configuration at high spin. Band 6 is tentatively assigned as the signature partner of band 5. These assignments provide a reasonable level of agreement between experiment and theory insofar as the relative positions of the configurations are reproduced. A more detailed discussion of the assignments and the ability of the CNS calculations to reproduce the observed data is presented below.

A. Bands 1 and 2

The Q_t values calculated as a function of spin within the CNS model are shown in Fig. 7(c). These predict that both the $\alpha=0$ and $\alpha=1$ signature partners of the $\langle 2,3\rangle$ configuration should show a decreasing trend in Q_t as the spin in-

TABLE III. Spins, γ-ray, and level energies, intensities of γ rays with initial state energy, spin and populated state spin for bands 5 and 6. The energies are given in keV.

${}_iI_n^\pi$	$E_{\rm lvl}$	E_γ	±	I_γ	±	${}_fI_n^\pi$	$R_{\rm DCO}$	±	$A_{\rm R}$	±
(9_1^+)	1447	103.7	0.1	30.7	1.2	(8_1^-)	0.51	0.02	1.25	0.04
(11_1^+)	2496	311.1	0.1	19.4	0.7	(10_1^-)	0.81	0.03	1.28	0.03
		1049.4	0.1	34.1	1.2	(9_1^+)	1.26	0.03	0.74	0.03
(13_1^+)	3628	299.2	0.1	7.9	0.3	(12_1^-)			1.33	0.05
		1131.4	0.1	45.8	1.5	(11_1^+)				
(14_1^+)	5652	1449.0	0.6	2.6	0.2	(13_1^-)				
(15_1^+)	4884	171.4	0.1	3.2	0.1	(14_2^-)			1.23	0.04
		1256.2	0.1	29.9	1.0	(13_1^+)	1.22	0.05	1.11	0.03
(16_1^+)	7103	1451.0	0.8	1.2	0.2	(14_1^+)				
(17_1^+)	6262	1378.0	0.1	26.0	0.9	(15_1^+)				
(18_1^+)	8752	1649.1	1.0	0.9	0.1	(16_1^+)				
(19_1^+)	7874	1611.7	0.1	11.8	0.5	(17_1^+)	1.17	0.04	1.00	0.03
(20_1^+)	10542	1769.0	0.4	0.4	0.1	(18_1^+)				
(21_1^+)	9816	1942.3	0.2	5.8	0.3	(19_1^+)	1.05	0.06	1.23	0.03
(22_1^+)	12534	1991.4	1.6	0.6	0.1	(20_1^+)			1.07	0.04
(23_1^+)	11843	2027.0	0.3	3.5	0.1	(21_1^+)			1.29	0.03
(25_1^+)	13936	2092.4	0.4	2.5	0.2	(22_1^+)			0.85	0.02
(27_1^+)	16230	2294.0	0.8	0.9	0.1	(25_1^+)			1.22	0.04
(29_1^+)	18806	2575.8	2.4	0.2	0.1	(27_1^+)				

creases and that the $\alpha=0$ structure should have a lower absolute value than its signature partner. The experimental results for bands 1 and 2, including the magnitude of the experimentally deduced Q_t around $I\sim 20$, are consistent with the calculations.

In nuclei, it is common that one signature of a configuration is "favored," or lower in energy, with respect to the other. The scaled energy difference between one signature of a given configuration with respect to the other is plotted as $(E_{(I)}-E_{(I-1)})/2I$ in Fig. 8(c) as a function of I. Normally this quantity increases with spin due to the action of the Coriolis force, but in Fig. 8(c) we can see that for bands 1 and 2 there is a "signature crossing" or "signature inversion" at $I=(15^-)$. In cases where high-j particles are involved such signature splittings have variously been described in terms of triaxial deformations [25] or the residual interaction between high-j particles [26,27]. In the case of ^{72}Br, the parity is negative which means that only one $g_{9/2}$ particle is involved. The signature crossing/inversion was observed in previous work [2] and was reproduced by CNS calculations in which a self-consistent deformation was calculated independently for each state. These deformations suggested an evolution from a triaxially deformed shape with rotation about the medium axis ($\gamma=-10°$ to $-15°$) at low spin to rotation about the small axis ($\gamma=+15°$ to $+20°$) at high spins. It was noted that this shape evolution was a requirement for the CNS calculations to reproduce the observed signature inversion.

Our $-1\hbar$ reassignment to bands 1 and 2 means that at low spins the $\alpha=1$ signature is now higher in energy than the $\alpha=0$ and vice versa at higher spins. This is opposite to the results obtained in the CNS calculations. However, we note that since the calculations were performed without pairing one might expect that they fail to describe the detailed features at low to intermediate spins. On the other hand, one could reasonably expect better agreement between experiment and calculations for $I=15-25$. Thus, under the assumption that the present spin assignments are correct, further work is clearly needed to see if other theoretical approaches

TABLE IV. Spins, γ-ray and level energies, intensities of γ rays with initial state energy, and spin and populated state spin for non-grouped states. The energies are given in keV.

${}_iI_n^\pi$	$E_{\rm lvl}$	E_γ	±	I_γ	±	${}_fI_n^\pi$	$R_{\rm DCO}$	±	$A_{\rm R}$	±
(2_1^-)	131									
(2_1^+)	124	124.0	1.0	11.4	1.1	(3_1^+)			1.41	0.03
(3_1^-)	218	86.7	0.1	13.7	1.1	(1_1^-)			1.82	0.07
(3_1^+)	0									
(4_1^+)	229	228.6	0.1	9.1	1.1	(3_1^+)	0.80	0.05	1.29	0.09
(4_1^-)	403	184.4	0.1	1.9	0.6	(3_1^-)			1.11	0.04
(3_2^+)	289	289.0	0.1	24.3	1.1	(3_1^+)	0.79	0.05	1.00	0.02
(5_1^-)	467	249.2	0.1	26.7	0.9	(3_1^-)			1.06	0.02
		135.9	0.3	3.2	0.1	(3_2^-)	0.84	0.04		
(5_1^+)	544	254.4	0.1	8.6	0.5	(3_2^+)	0.98	0.04	1.25	0.07
(5_2^-)	748	346.0	0.2	2.4	0.1	(4_1^-)	0.86	0.06	0.74	0.02
		416.2	0.3	2.2	0.1	(3_2^-)			0.70	0.02
(6_1^-)	716	248.0	0.1	13.4	1.4	(5_1^-)			1.06	0.02
(7_2^-)	1187	471.1	0.1	14.4	0.4	(6_1^-)	0.73	0.14	0.92	0.03
		528.8	0.1	7.5	0.2	(5_2^-)			0.60	0.03
$(?_?^?)$	5361	1156.0	0.2	9.8	0.5	(13_1^-)				
$(?_?^?)$	8088	1847.3	0.2	3.0	0.2	(16_1^-)				

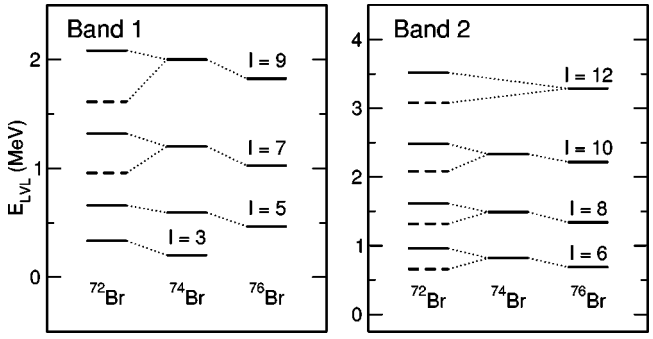

FIG. 5. Comparisons between states in bands 1 and 2 of ^{72}Br to equivalent states in ^{74}Br [11,12] and ^{76}Br [13–15]. Solid lines represent the energy of each state and dotted lines connect states of the same spin in each isotope. The dashed lines indicate the positions of states in ^{72}Br under assignments made in previous work [2].

can describe this phenomenon. It is interesting to note that in very recent work [28] it is suggested that the signature inversion in the positive-parity yrast band of ^{84}Rb may be understood if the quadrupole deformation is assumed to be prolate below the inversion point, triaxial at the inversion, and oblate above it.

The large signature splitting at high spins in bands 1 and 2 [Fig. 8(a) above $I^{\pi}=24^{-}$] is not reproduced by the CNS calculations. However, they do correctly predict that the $\alpha=1$ signature should be the lowest at the highest spins.

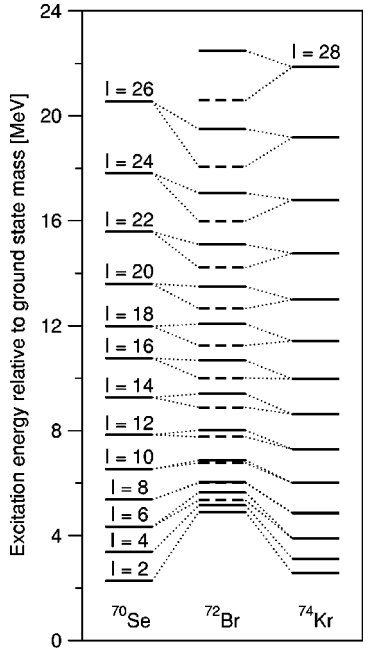

FIG. 6. Comparisons between even-spin, yrast states (regardless of parity) in ^{72}Br, ^{70}Se [19], and ^{74}Kr [20]. States in ^{70}Se, ^{72}Br, and ^{74}Kr have been adjusted by 1.330 MeV, 4.687 MeV, and 2.111 MeV, respectively, so that they are all plotted relative to the even-nucleus energy at the spherical shape of the FRDM [16]. Solid lines represent the energy of each state and dotted lines connect states of the same spin in each nucleus. The dashed lines indicate the positions of states in ^{72}Br under assignments made in previous work [2].

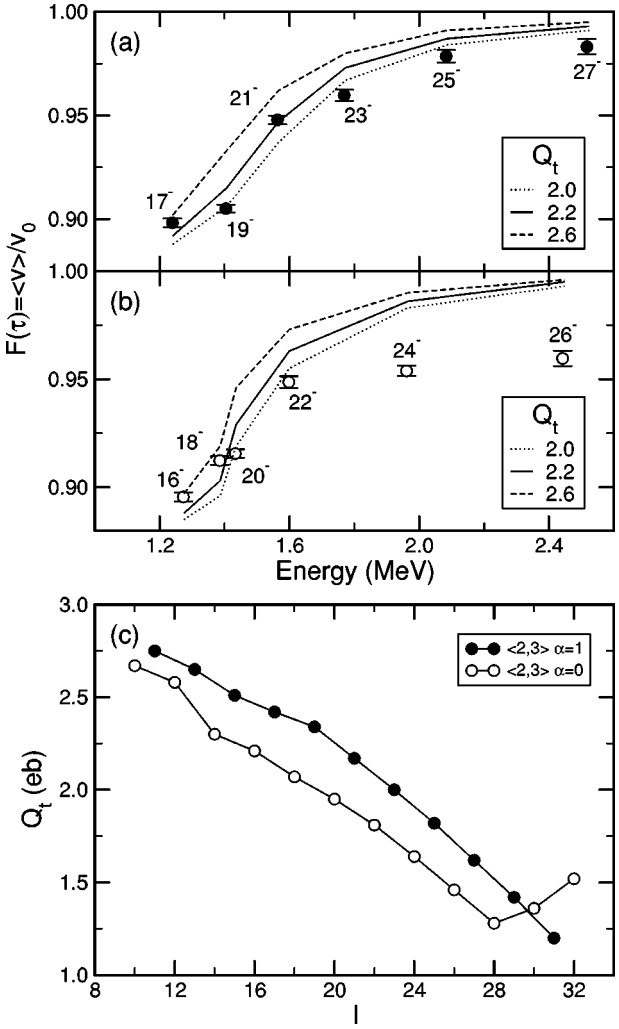

FIG. 7. F(τ) curve for bands in ^{72}Br. Experimental points are symbols only. Representative curves from STIME [22] are shown as lines with corresponding Q_t indicated in the legend. Points are marked with the spin and parity of the state, the appropriate γ ray deexcites. For (a) band 1, (b) band 2. (c) CNS predictions for Q_t as a function of spin for both bands.

Figure 9 shows the $\mathfrak{I}^{(1)}$ moment of inertia for all three structures as a function of the rotational frequency squared, ω^2. The agreement between experiment and theory is clearly excellent for bands 1 and 2 at high rotational frequencies.

B. Bands 3 and 4

A possible assignment for bands 3 and 4 is a $\langle 3,4\rangle$ configuration as suggested in Fig. 8. In a recent conference publication [29] the existence of two $\langle 3,4\rangle$ configurations in ^{72}Br is discussed. The first has a lower deformation ($\varepsilon_2 \sim 0.28$) and is the configuration shown in Fig. 8(b). The second has a similar configuration, but also involves two proton and one neutron hole in the strongly up-sloping (as a function of quadrupole deformation) $f_{7/2}$ orbital. This configuration has a broken ^{56}Ni core and a larger deformation ($\varepsilon_2 \sim 0.38$). This is referred to as the $\langle 3,4\rangle$* configuration [29]. The disappearance of the signature splitting near I

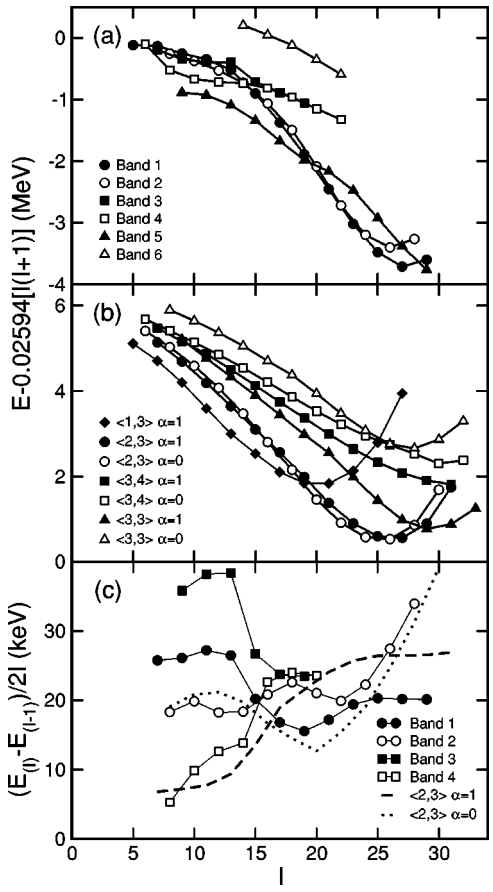

FIG. 8. Level energies relative to a rotational liquid drop reference energy for (a) experimental data. (b) Results from CNS calculations. (c) Plot of signature-splitting vs spin for bands 1, 2, 3, and 4 with a comparison to CNS calculations for bands 1 and 2.

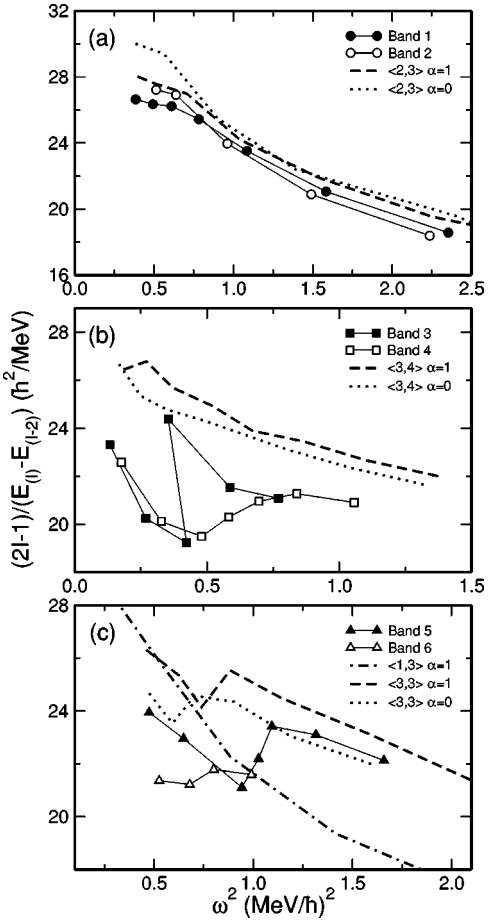

FIG. 9. (a) Plot of $\mathfrak{I}^{(1)}=(2I-1)/(E_{(I)}-E_{(I-2)})$ vs angular frequency $\omega=(E_{(I)}-E_{(I-2)})/2$ squared for bands 1 and 2. (b) For bands 3 and 4. (c) For bands 5 and 6. Experimental data are symbols and solid lines, results from CNS calculations are shown as dotted, dashed, and dot-dashed lines.

$=(16)$ may indicate that bands 3 and 4 evolve from a $\langle 3,4\rangle$ configuration at low spin to the $\langle 3,4\rangle$* configuration at higher spins, where the zero signature splitting is determined by the $f_{7/2}$ neutron orbital. We note, however, that at low spins the $\alpha=1$ signature of the $\langle 3,4\rangle$ configuration is predicted to be lowest in energy from the CNS calculations, while experimentally it is the $\alpha=0$ signature that is the lowest and hence there is some discrepancy between the CNS calculations and experiment at low spins. It would clearly be useful to have lifetime data for these states in order to be able to check the tentative assignments above. If the interpretation is correct one would expect a significant enhancement in the deformation for both bands above $I=(16)$. Figure 9(b) shows a modest level of agreement between the shape of the experimental and theoretical $\mathfrak{I}^{(1)}$ moments of inertia for bands 3 and 4 at high rotational frequencies.

C. Bands 5 and 6

From the present work we believe that the previous assignment of a $\langle 1,3\rangle$ configuration to band 5 cannot be correct at high spin because the $\langle 1,3\rangle$ configuration has a maximum spin $I_{max}=27$. In the present work this structure is not calculated to terminate at $I=27$ because of the strong coupling between the different subshells at high rotational frequencies. However, the $I=27,29$ states of the $\langle 1,3\rangle$ configuration are calculated to reside so high in excitation energy that we believe that band 5 cannot have this configuration for these spin values. Instead, a comparison between the data and the CNS calculations (see Fig. 8) suggests that band 5 has a $\langle 3,3\rangle$ configuration at high spin. The change in slope in the calculations for this configuration near spin $I=(21)$ in the $\alpha=1$ band corresponds to a change in triaxial deformation from $-15°$ to $+15°$. The experimental data clearly show a similar behavior at around the same spin, suggesting that the predicted shape change for this configuration may be observed experimentally. However, it is more likely that the observed change in slope in Fig. 7(a) is due to a configuration change from $\langle 1,3\rangle$ (at low spins) to $\langle 3,3\rangle$ (at high spins). This latter proposal gains further support from the behavior of the $\mathfrak{I}^{(1)}$ values shown in Fig. 9(c).

The CNS calculations in Fig. 8(b) provide tentative evidence in support of assigning band 6 to be the signature partner of band 5. This is based on the fact that the energy splitting between the two bands is comparable in both the calculations and the experimental data. However, the fact

that band 6 prefers to decay to a negative-parity structure (band 1) clearly detracts from this argument somewhat.

V. SUMMARY

In summary, we have investigated high-spin states in ^{72}Br. A total of six rotational bands have been observed. They have been grouped into three signature partner split bands with configuration assignments of $\langle 2,3\rangle$ for bands 1 and 2, $\langle 3,4\rangle$ for bands 3 and 4, and $\langle 1,3\rangle$ for band 5 at low spin, evolving to a $\langle 3,3\rangle$ configuration at high spin. A sixth band is tentatively assigned as the signature partner of band 5. We note that while the CNS model appears to have some success in explaining the observed bands and their properties, it also has some problems. This is particularly intriguing as the model has worked well for other nuclei in this region (e.g., the isotone ^{73}Kr [30] and isotope ^{73}Br [3]). We have found several differences between our level scheme and that proposed in a previous work—most significantly with the previously observed $\langle 2,3\rangle$ structure, which we suggest is one unit of spin lower than hitherto thought. The new assignment has far better agreement with the expected systematics. This mandates further investigation into the description of the signature inversion observed in this structure. Additional work, using a range of theoretical approaches, is desirable in order to try and understand the properties of the observed bands and to confirm their configurations. This nucleus would appear to provide a challenging testing ground for state-of-the-art nuclear structure models.

ACKNOWLEDGMENTS

This work has been partially supported by the UK EPSRC, the NSERC of Canada, the Swedish Research Council, and the U.S. DOE under Contract Nos. DE-FG02-95ER-40934, DE-AC02-76SF-00098, DE-FG02-88ER-40406, and W-31-109-ENG38.

[1] D. G. Jenkins *et al.*, Phys. Rev. C **65**, 064307 (2002).
[2] C. Plettner *et al.*, Phys. Rev. Lett. **85**, 2454 (2000).
[3] C. Plettner *et al.*, Phys. Rev. C **62**, 014313 (2000).
[4] G. Garcia Bermudez, C. Baktash, A. J. Kreiner, and M. A. J. Mariscotti, Phys. Rev. C **25**, 1396 (1982).
[5] S. Ulbig, F. Cristancho, J. Heese, K. P. Lieb, T. Osipowicz, B. Wörmann, J. Eberth, T. Mylaeus, and M. Wiosna, Z. Phys. A **329**, 51 (1988).
[6] N. Fotiades *et al.*, Phys. Rev. C **60**, 057302-1 (1999).
[7] I. Y. Lee, Nucl. Phys. **A520**, 641c (1990).
[8] D. G. Sarantites, P-F. Hua, M. Devlin, L. G. Sobotka, J. Elson, J. T. Hood, D. R. LaFosse, J. E. Sarantites, and M. R. Maierb, Nucl. Instrum. Methods Phys. Res. A **381**, 418 (1996).
[9] D. G. Sarantities, http://www.chemistry.wustl.edu/ dgs/ NeutronShell/NeutronShell.html
[10] K. S. Krane, R. M. Steffen, and R. M. Wheeler, Nucl. Data Tables **11**, 351 (1973).
[11] J. Doring, J. W. Holcomb, T. D. Johnson, M. A. Riley, S. L. Tabor, P. C. Womble, and G. Winter, Phys. Rev. C **47**, 2560 (1993).
[12] J. W. Holcomb, T. D. Johnson, P. C. Womble, P. D. Cottle, S. L. Tabor, F. E. Durham, and S. G. Buccino, Phys. Rev. C **43**, 470 (1991).
[13] D. F. Winchell, J. X. Saladin, M. S. Kaplan, and H. Takai, Phys. Rev. C **41**, 1264 (1990).
[14] S. G. Buccino, F. E. Durham, J. W. Holcomb, T. D. Johnson, P. D. Cottle, and S. L. Tabor, Phys. Rev. C **41**, 2056 (1990).
[15] J. D. öring, G. Winter, L. Funke, P. Kemnitz, and E. Will, Z. Phys. A **305**, 365 (1982).
[16] P. Möller, J. R. Nix, W. D. Myers, and W. J. Swiatecki, At. Data Nucl. Data Tables **59**, 185 (1995).
[17] I. Ragnarsson, Z. Xing, T. Bengtsson, and M. A. Riley, Phys. Scr. **34**, 651 (1986).
[18] I. Ragnarsson *et al.* (unpublished).
[19] G. Rainovski *et al.*, J. Phys. G **28**, 2617 (2002).
[20] D. Rudolph *et al.*, Phys. Rev. C **56**, 98 (1997).
[21] B. Cederwall *et al.*, Nucl. Instrum. Methods Phys. Res. A **354**, 591 (1995).
[22] J. F. Zeigler, J. P. Biersac, and U. Littmark, *The Stopping and Ranges of Ions in Matter* (Pergamon, London, 1985), Vol. I.
[23] A. V. Afanasjev, D. B. Fossan, G. Lane, and I. Ragnarsson, Phys. Rep. **322**, 1 (1999).
[24] D. Galeriu, D. Bucurescu, and M. Ivasku, J. Phys. G **12**, 329 (1986).
[25] R. Bengtsson, H. Frisk, F. R. May, and J. A. Pinston, Nucl. Phys. **A415**, 189 (1984).
[26] P. B. Semmes and I. Ragnarsson, in *Proceedings of the Conference on High Spin Physics and Gamma-soft Nuclei, Pittsburg, 1990*, edited by J. X. Saladin, R. A. Sorensen, and C. M. Vincent (World Scientific, Singapore, 1991), p. 500; in *Proceedings of the Conference on Future Directions in Nuclear Physics with 4π Detector Systems of the New Generation, Strasbourg, 1991*, edited by J. Dudek and B. Haas (AIP, New York, 1992), p. 556.
[27] R. A. Bark *et al.*, Nucl. Phys. **A630**, 603 (1998).
[28] S. Shen, J. Gu, S. Shi, J. Liu, J. Zhou, and W. Shen, Phys. Lett. B **554**, 115 (2003).
[29] N. S. Kelsall *et al.* (unpublished).
[30] N. S. Kelsall *et al.*, Phys. Rev. C **65**, 044331-1 (2002).